Coordination Chemistry Reviews, 11 (1973) 247–262

PARTIAL QUADRUPOLE SPLITTINGS IN INORGANIC CHEMISTRY

G.M. BANCROFT*

Chemistry Department, University of Western Ontario, London 72 (Canada)

(Received February 7th, 1973)

CONTENTS

A. INTRODUCTION

The Mössbauer effect (or nuclear gamma resonance)[1] has been observed for over 30 elements. Of the 23 main group and transition elements which exhibit the effect[2,3], only two isotopes, ^{57}Fe and ^{119}Sn, are easily used for routine work outside a specialist's laboratory. However, chemical information of considerable interest has been obtained[4] for a number of other isotopes such as ^{99}Ru, ^{121}Sb, ^{125}Te, ^{127}I, ^{129}I, ^{129}Xe, ^{182}W, ^{193}Ir and ^{197}Au.

In this article, I am going to discuss mainly the partial quadrupole splitting (PQS) treatment[5–7] and how this expands the use of Mössbauer spectroscopy in inorganic chemistry in three major directions. First, the PQS treatment leads to elucidation of structure in Fe and Sn compounds, and also in compounds containing other isotopes which exhibit either nuclear gamma resonance or nuclear quadrupole resonance (NQR). Second, the PQS treatment enables calculation of quadrupole parameters for other Mössbauer and NQR isotopes such as ^{99}Ru, ^{55}Mn and ^{59}Co. Thirdly, the treatment leads to estimation of bonding properties of ligands which has led to preparation of new compounds. Before looking at these applications, I will emphasize the more correlative uses of the PQS model in rationalizing ^{57}Fe and ^{119}Sn quadrupole splittings.

* This article is taken largely from the 1971 Meldola Lecture presented in September 1972 in Nottingham, England.

It is well worth keeping in mind the main criteria of any good chemical model, and I will try to demonstrate how this PQS treatment fulfills these criteria. First, the model should correlate known experimental information; second, through the model, we should gain insight into bonding and structure; and third, the model should lead to prediction of other results which provide impetus for new experiments. The uses of the PQS values mentioned in the last paragraph span these three criteria.

B. BASIC THEORY FOR MÖSSBAUER SPECTROSCOPY

Mössbauer spectroscopy can be readily compared with other resonant spectroscopic experiments such as ultra-violet spectroscopy. In Mössbauer spectroscopy, we consider transitions between *nuclear* energy levels with emission and absorption of *gamma* rays; in UV spectroscopy, we of course consider transitions between *electronic* energy levels with emission and absorption of UV radiation. In Mössbauer spectroscopy, a radioactive source is used, and the source is vibrated to provide the means of energy scanning via the well known Doppler effect.

$$\Delta E = (v/c)E_\gamma$$

As in most resonant experiments we plot absorption versus energy (Fig.1) (velocity in this case) and obtain a very simple spectrum for a powder sample in the Fe and Sn case. Two

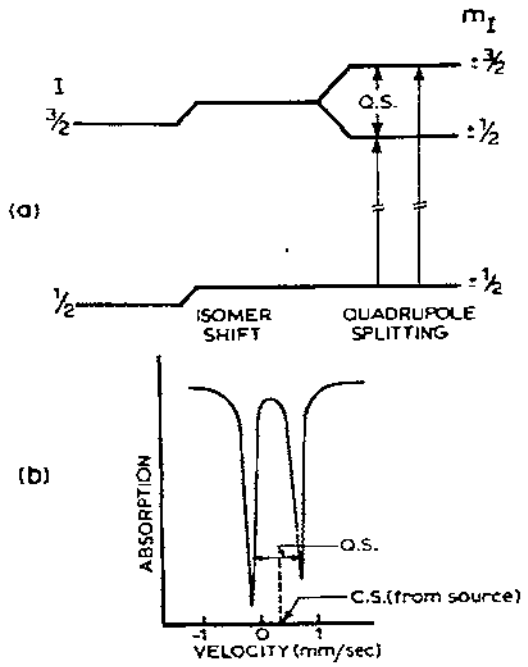

Fig.1. Nuclear energy levels. (a) The isomer or center shift and quadrupole splitting for $I_{gr} = \frac{1}{2}, I_{ex} = \frac{3}{2}$. (b) Resultant Mössbauer spectrum.

peaks are obtained, and two parameters extracted; the isomer shift or center shift (CS) and the quadrupole splitting (QS).

The dominant term in the centre shift can be expressed[8,9] as

$$CS \propto \delta R/R \; [\psi(0)_s]^2_{\text{absorber}} \tag{1}$$

For ^{57}Fe, since $\delta R/R$ is negative, the CS decreases as $[\psi(0)_s]^2$ increases. The CS is also sensitive to valence orbital changes, and decreases as the 4s population increases and 3d population decreases (due to deshielding)[4].

The quadrupole splitting results from a splitting of the $\frac{3}{2}$ level from a non-zero electric field gradient (EFG) at the Mössbauer atom (Fig.1). The field gradient is a 3 X 3 tensor (Table 1) which for point charges Z_i a distance r_i from the Mössbauer atom can be expressed as given in Table 1.

TABLE 1
The electric field gradient (EFG) tensor

$$EFG = -\begin{bmatrix} V_{xx} & V_{xy} & V_{xz} \\ V_{yx} & V_{yy} & V_{yz} \\ V_{zx} & V_{zy} & V_{zz} \end{bmatrix}$$

$$V_{xx} + V_{yy} + V_{zz} = 0$$

$$V_{xx} = e \sum_i \frac{Z_i}{r_i^3} (3 \sin^2\theta_i \cos^2\phi_i - 1)$$

$$V_{yy} = e \sum_i \frac{Z_i}{r_i^3} (3 \sin^2\theta_i \sin^2\phi_i - 1)$$

$$V_{zz} = e \sum_i \frac{Z_i}{r_i^3} (3 \cos^2\theta_i - 1)$$

$$V_{xy} = V_{yx} = e \sum_i \frac{Z_i}{r_i^3} (3 \sin^2\theta_i \sin\phi_i \cos\phi_i)$$

$$V_{xz} = V_{zx} = e \sum_i \frac{Z_i}{r_i^3} (3 \sin\theta_i \cos\theta_i \cos\phi_i)$$

$$V_{yz} = V_{zy} = e \sum_i \frac{Z_i}{r_i^3} (3 \sin\theta_i \cos\theta_i \sin\phi_i)$$

This tensor is easily diagonalized for most cases of interest, but because it is traceless, there are just two independent components normally chosen to be q and η. θ is the angle from the Z EFG axis, and ϕ the angle from the X EFG axis. The quadrupole splitting (QS) for a $\frac{3}{2}$ nucleus can then be expressed as

$$QS = \tfrac{1}{2}e^2qQ(1+\eta^2/3)^{\frac{1}{2}} \tag{2}$$

where $q = V_{zz}/e$, $\eta = (V_{xx} - V_{yy})/V_{zz}$, Q = quadrupole moment (a nuclear constant), and e is the protonic charge. We can then divide q into two terms[10]

$$q = (1-R)q_{\text{valence}} + (1-\gamma_\infty)q_{\text{lattice}} \tag{3}$$

where R and γ_α are the Sternheimer antishielding factors, q_{lattice} is given by

$$q_{\text{lattice}} = \Sigma \frac{Z_i(3\cos^2\theta_i - 1)}{r_i^3} \tag{4}$$

and for p electrons, q_{valence} is given by[11]

$$q_{\text{valence}} = K_p[-N_{p_z} + \tfrac{1}{2}(N_{p_y} + N_{p_x})] \tag{5}$$

where K_p is a constant for a given p orbital in a given atom, and the N's are orbital populations. Both these terms are zero for cubic or higher (e.g. spherosymmetric) symmetry. Thus if $N_{p_z} = N_{p_x} = N_{p_y} = 2$ (as in I^-), $q_{\text{valence}} = 0$. If $N_{p_z} > \frac{1}{2}(N_{p_x} + N_{p_y})$, then a negative q is obtained; if $N_{p_z} < \frac{1}{2}(N_{p_x} + N_{p_y})$, a positive q is obtained. Thus a concentration of negative charge along the Z EFG axis gives a negative q (and negative QS if Q is positive), and the magnitude of q and the QS depends on the difference between N_{p_z} and $\frac{1}{2}(N_{p_x} + N_{p_y})$ often referred to as the p electron imbalance. Similarly for q_{lattice}, (Fig.2) if we have an octahedral distribution of point charges about the Mössbauer atom, then $q_{\text{lattice}} = 0$. If we compress the axial ligands along the Z axis, then q_{lattice} is negative and vice versa. Again, a concentration of negative charge along the Z axis gives a negative q, and the magnitude of q_{lattice} depends on the amount of distortion from octahedral symmetry. Although it is usually not possible to obtain the sign of e^2qQ from a random sample, both single crys-

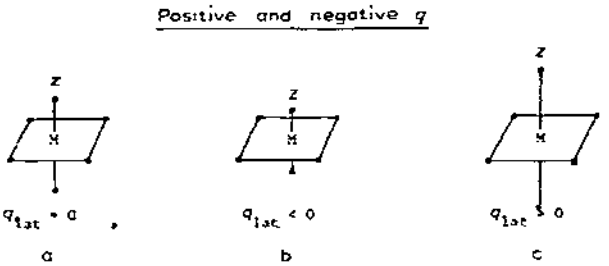

Fig.2. Representation of six point charges about a Mössbauer atom M and the sign of q. (a) Octahedral, $q_{\text{lat}} = 0$; (b) axial compression, $q_{\text{lat}} < 0$; (c) axial elongation, $q_{\text{lat}} > 0$.

tal[12] and magnetic field methods[13,14] enable the determination of the sign of many ^{57}Fe and ^{119}Sn quadrupole splittings[4]. In contrast, the sign of e^2qQ *cannot* be obtained from NQR measurements.

(i) The bonding of dinitrogen

It is interesting now to use the above qualitative concepts to obtain bonding information in Fe^{II} low spin compounds of the type *trans*-$[FeHL(depe)_2]^+BPh_4$ (depe = 1,2-bis-diethylphosphinoethane; L = RNC, CO, $P(OR)_3$, RCN, and N_2), and in particular to compare the bonding of the novel ligand N_2 with CO and other neutral ligands[15,16]. Considering the bonding in these compounds, σ donation by L populates the "$d_{z^2}\ sp_z$" hybrid orbital on the Fe, and π acceptance withdraws d_{xz} and d_{yz} electron density from metal to ligand. Both of these interactions increase the *s* electron density at the nucleus and decrease the CS

$$CS \propto -(\sigma + \pi) \tag{6}$$

In contrast, the quadrupole splitting is a measure of the differences in *d* orbital populations*

$$q_{\text{valence}} = K_d[-N_{d_{z^2}} + N_{d_{x^2-y^2}} + N_{d_{xy}} - \tfrac{1}{2}(N_{d_{xz}} + N_{d_{yz}})] \tag{7}$$

For *trans*-$[FeHL(depe)_2]^+$, the *Z* EFG axis lies along the pseudo-fourfold molecular axis, and as the σ donor strength of L increases, $N_{d_{z^2}}$ increases giving a more negative q; as the π acceptor properties of L increase, $N_{d_{xz}} + N_{d_{yz}}$ decreases and q becomes more positive.

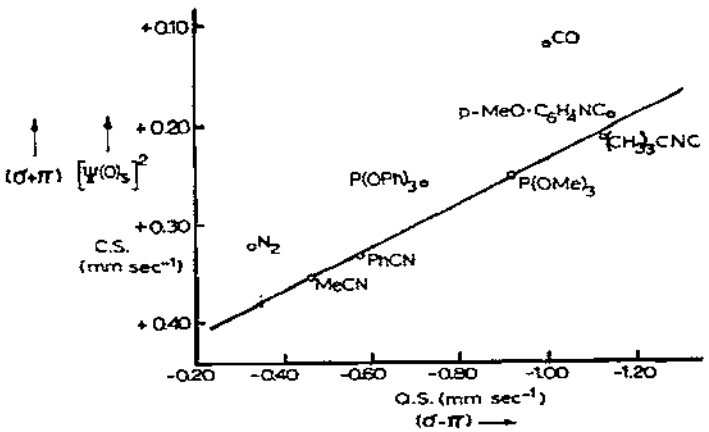

Fig.3. Plot of CS versus QS for the series of compounds *trans*-$[FeHL(depe)_2]^+BPh_4^-$ (L = N_2, MeCN, PhCN, $P(OPh)_3$, $P(OMe)_3$, $PMeO{\cdot}C_6H_4{\cdot}NC$, $(CH_3)_3CNC$, CO). The trend in $(\sigma + \pi)$ and $(\sigma - \pi)$ is noted.

* We neglect the much smaller contribution from a 4*p* electron imbalance.

Thus

$$q \text{ (and QS)} \propto (\pi - \sigma) \tag{8}$$

Potentially then, eqns. (6) and (8) could be used to separate relative σ and π for these ligands. If we plot CS versus QS (Fig.3), then except for N_2 and CO there is a reasonable linear correlation with a positive slope indicating that σ effects are dominant in determining both the CS and QS. That N_2 and CO (and $P(OPh)_3$ to a smaller extent) lie significantly to the left of the line, indicates that π acceptance is relatively much more important for these two ligands than for the others. The CS indicates then that N_2 is a weak $\sigma + \pi$ ligand, comparable to CH_3CN; but the QS indicates that N_2 is an appreciably better π acceptor and/or poorer σ donor that nitriles. Thus we conclude that N_2 is a very weak σ donor but moderate π acceptor[16], and this result is consistent with other predictions[17]. CO and isocyanides are very strong ($\sigma + \pi$) ligands, but CO is a much stronger π acceptor than isocyanides.

C. PARTIAL QUADRUPOLE SPLITTINGS

(i) Introduction and assumptions

Taking each ligand to represent a point charge Z_i, we can write the components of the EFG tensor as in Table 2. The [L] values are termed partial field gradients. In this model, we make four rather drastic assumptions (over and above the point charge approximation).

TABLE 2
EFG components expressed in terms of partial field gradients [L]

$$V_{xx} = e \Sigma_L [L] (3 \sin^2\theta_L \cos^2\phi_L - 1)$$

$$V_{yy} = e \Sigma_L [L] (3 \sin^2\theta_L \sin^2\phi_L - 1)$$

$$V_{zz} = e \Sigma_L [L] (3 \cos^2\theta_L - 1)$$

$$V_{xy} = V_{yx} = e \Sigma_L 3[L] \sin^2\theta_L \sin\phi_L \cos\phi_L, \text{ etc.}$$

where

$$[L] = \frac{Z_L}{r_L^3}$$

(1) We assume that the QS can be regarded as a sum of independent contributions, one from each ligand bound to the metal atom.

(2) We assume that the partial field gradients (and also the partial quadrupole splittings) are constants from one compound to another for one Mössbauer isotope in a given electronic state and coordination number, e.g. six-coordinate Fe^{II} or four-coordinate Sn^{IV}.

(3) We assume that all bond angles are ideal, i.e. that in the octahedral case all L–M–L bond angles are 90°.

(4) We assume that the principal EFG axes correspond in the octahedral case, to metal ligand bond directions and in many other cases to molecular symmetry axes.

Structural studies indicate that six coordinate transition metal species are usually close to octahedral (the L–M–L bond angles[18] are 90° ± 8°), and NQR studies have shown usually that the EFG axes correspond closely to metal ligand bond directions [19,20].

Applying the point charge approximation and the above assumptions, the expressions for the EFG components for *trans*-FeA_2B_4 are easily derived (Table 3), and the quadrupole splitting is then given by a simple difference of partial quadrupole splittings, i.e. $QS = 4(PQS)_A - 4(PQS)_B$. For *cis*-FeA_2B_4 and $FeAB_5^+$ species, the expressions for V_{zz}/e ($\eta = 0$ in all cases) are given in Table 4 and it is apparent that the predicted ratio of *trans* : *cis* : $FeAB_5^+ = 2 : -1 : 1$. The observed quadrupole splittings for A = Cl and B = ArNC are in excellent agreement with the predicted* values.

TABLE 3
Point charge EFG expressions for *trans*-FeA_2B_4

V_{XX}/e	$= -2[A] + 2[B]$
V_{YY}/e	$= -2[A] + 2[B]$
V_{ZZ}/e	$= 4[A] - 4[B]$
η	$= 0$
QS	$= \frac{1}{2}eV_{ZZ}Q$
	$= \frac{1}{2}e^2Q\,(4[A] - 4[B])$
or QS	$= 4(PQS)_A - 4(PQS)_B$

where

$(PQS)_A$	$= \frac{1}{2}e^2Q\,[A]$

TABLE 4
Predicted and observed[5,21] quadrupole splittings for *trans*-FeA_2B_4, *cis*-FeA_2B_4, and $FeAB_5^+$

Structure	V_{ZZ}/e	Ratio
trans-FeA_2B_4	$4[A] - 4[B]$	2
cis-FeA_2B_4	$-2[A] + 2[B]$	−1
$[FeAB_5]^+$	$2[A] - 2[B]$	1
trans-$FeCl_2(ArNC)_4$	QS = +1.55 mm.sec^{-1}	
cis-$FeCl_2(ArNC)_4$	QS = −0.78 mm.sec^{-1}	
$[FeCl(ArNC)_5]^+ClO_4$	QS = 0.73 mm.sec^{-1}	

* The sign of the QS for $[FeCl(ArNC)_5]^+ClO_4$ has not yet been measured. Wherever sign are not quoted, they have not yet been obtained.

More generally, we would like to calculate one PQS value from which we can derive a whole table of PQS values from compounds of known structure. For example, Cl^- has been assigned[5] a PQS value of -0.30 mm.sec^{-1}, and $(PQS)_{ArNC}$ can then be obtained from *trans*-$FeCl_2(ArNC)_4$ (compound 1, Table 5). Thus $+1.55 = -1.20 - 4(PQS)_{ArNC}$ and $(PQS)_{ArNC} = -0.69$ mm.sec^{-1}. Using PQS values derived in this way (Table 6), we can predict the quadrupole splittings for a large number of compounds, some of which are given in Table 5.

TABLE 5
Predicted and observed QS (mm.sec^{-1}) at 295°K

	Observed	Predicted
1 *trans*-$FeCl_2(ArNC)_4$	+1.55	
2 *cis*-$FeCl_2(ArNC)_4$	−0.78	−0.78
3 $[FeCl(ArNC)_5]ClO_4$	0.73	+0.78
4 *trans*-$Fe(SnCl_3)_2(ArNC)_4$	+1.05	
5 *cis*-$Fe(SnCl_3)_2(ArNC)_4$	0.50	−0.52
6 *cis*-$FeClSnCl_3(ArNC)_4$	0.61	−0.69 ($\eta = 0.60$)
7 *trans*-$FeH_2(depb)_2$	−1.84	
8 *trans*-$FeHCl(depe)_2$	<0.12	−0.20
9 *trans*-$Fe(EtNC)_4(CN)_2$	−0.60	
10 *cis*-$Fe(EtNC)_4(CN)_2$	0.29	+0.30
11 *trans*-$[FeH(ArNC)(depe)_2]BPh_4$	−1.14	−0.98
12 *trans*-$[FeH(CO)(depe)_2]BPh_4$	1.00	−0.46

TABLE 6
Partial quadrupole splittings for Fe^{II} (mm.sec^{-1}) at 80°K[a]

Ligand	PQS value	Ligand	PQS value
NO^{+*}	+0.01	$P(OPh)_3$	−0.55
X^-	−0.30	CO	−0.55
N_2	−0.37	PPh_2Et	−0.58
N_3^-	−0.38	PPh_2Me	−0.58
CH_3CN	−0.43	depb/2	−0.59
$SnCl_3^-$	−0.43	$P(OEt)_3$	−0.63
H_2O^*	−0.45	depe/2	−0.65
$SbPh_3$	−0.50	$P(OMe)_3$	−0.65
NCS^-	−0.51	PMe_3	−0.66
$AsPh_3$	−0.51	dmpe/2	−0.70
NH_3^*	−0.52	ArNC	−0.70
NCO^-	−0.52	CN^{-*}	−0.84
PPh_3	−0.53	H^-	−1.04

[a] Ref. 22. Those ligands asterisked had their PQS values derived from room temperature data.

Except for compound 12 in Table 5, the predicted quadrupole splittings are in excellent agreement with the observed values. The great majority of our observed quadrupole splittings[22] and those observed by other groups[23] are within 0.20 mm.sec^{-1} of the predicted values, and we feel that 0.20 mm.sec^{-1} can be considered as good agreement. For strong π acceptor ligands such as CO the PQS treatment might not be expected to work as well[24] (compound 12, Table 5), but agreement between predicted and observed Fe^{II}–CO compounds is generally satisfactory[22]. The PQS values in Table 6 have been calculated using 80°K data, because more compounds have now been run at that temperature. Using these PQS values, we can now predict and rationalize Fe^{II} low spin quadrupole splittings for compounds containing these ligands in any combination.

Similarly, for Sn^{IV} compounds in both octahedral and tetrahedral geometries, PQS value can be derived[6,24,25] (Table 7) and once again these PQS values are very successful in predicting quadrupole splittings but somewhat less successful in predicting η values (Table 8). η and the sign of the quadrupole splitting are much more sensitive to the assumptions than the |QS|[27], and the signs for *cis* octahedral Sn^{IV} compounds are often the same as those for the corresponding *trans* isomer[28,29].

TABLE 7

Partial quadrupole splittings for four-coordinate Sn^{IV} (refs. 21, 24)

Ligand	PQS
X (F, Cl, Br)	0.00
C_6F_5	−0.76
$Mn(CO)_5$	−0.97
$Fe(CO)_2C_5H_5$	−1.08
C_6H_5	−1.26
CH_3, C_2H_5	−1.37

TABLE 8

Predicted and observed values of e^2qQ and η for four-coordinate Sn^{IV} compounds[25,26]

Compound	QS		η	
	Calc.	Obs.	Calc.	Obs.
1 $Me_3SnMn(CO)_5$		−0.80		
2 $Me_2ClSnMn(CO)_5$	−2.59	−2.60	0.41	0.35
3 $MeCl_2SnMn(CO)_5$	+2.79	+2.62	0.89	0.46
4 $Cl_3SnMn(CO)_5$	+2.16	+1.83	0.00	~ 0
5 $Ph_3SnMn(CO)_5$	−0.58	0.41	0.00	
6 $Ph_2ClSnMn(CO)_5$	−2.39	2.50	0.32	
7 $PhCl_2SnMn(CO)_5$	+2.62	2.52	0.94	
8 $Ph_2(C_6F_5)SnMn(CO)_5$	−0.97	0.95	0.78	
9 $Ph(C_6F_5)_2SnMn(CO)_5$	+0.95	1.06	0.58	
10 $(C_6F_5)_3SnMn(CO)_5$	+0.42	+0.99	0.00	

Despite these discrepancies (caused by the very distorted *cis* structures[28]) the predicted and observed quadrupole splittings for a very large number of octahedral and tetrahedral Sn^{IV} compounds[4,24] are in good agreement.

(ii) Structure

The simplest use of the $2:-1$ ratio is to assign *cis* and *trans* isomers in Fe^{II} (refs. 5, 30) and Sn^{IV} (refs. 6, 31) compounds. In many cases, this assignment is difficult to make by other spectroscopic techniques. For example in Table 9, *cis* and *trans* structures can be assigned immediately. The assignment of the $P(OMe)_3$ isomers has been very important in the interpretation[32] of the surprising ^1H NMR spectrum of *cis*-$Fe(NCS)_2[P(OMe)_3]_4$. This spectrum consists of two sharp indistinguishable triplets, one assigned to the *trans*-$P(OMe)_3$ pair and the other to the *cis*-$P(OMe)_3$ pair. This represents the first example of two virtual triplets from one molecule.

TABLE 9
Quadrupole splittings ($mm.sec^{-1}$) for *cis*–*trans* isomers[21,30,32]

trans-$Fe(CN)_2(EtNC)_4$	−0.60
cis-$Fe(CN)_2(EtNC)_4$	(+)0.30
trans-$FeCl_2(ArNC)_4$	+1.55
cis-$FeCl_2(ArNC)_4$	−0.78
trans-$Fe(NCS)_2[P(OMe)_3]_4$	(+)0.56
cis-$Fe(NCS)_2[P(OMe)_3]_4$	(−)0.30

Partial quadrupole splittings are however, of greater predictive use for assignment of more complex structures[22]. For example, if we take the five geometric isomers of $Fe(CO)_2[P(Me)_3]_2I_2$ (Table 10), the predicted QS values are generally very different. The two isomers made to date give QS in excellent agreement with those predicted. From the CO infrared and the quadrupole splitting, any of these isomers can now be assigned.

Finally in this section, the most important structural use of PQS values is in the assignment of structure to Sn^{IV} compounds. Many Sn^{IV} compounds have associated five- and six-coordinate structures. Association causes a large increase in quadrupole splitting from the unassociated four-coordinate structure, as predicted by the PQS treatment[6,24,33]. For example, the larger QS for Me_3SnX (X = F, Cl, Br, I) (Table 11) strongly suggest a five-coordinate associated structure, as has been observed by X-ray studies on Me_3SnF (ref. 34) and Me_3SnCl (ref. 35). The much smaller QS values for Ph_3SnX (X = Cl, Br, I) strongly suggest an unassociated four-coordinate structure[24,33] and this has been confirmed recently by an X-ray study[36]. Similarly, Me_2SnCl_2 has a much larger QS than Ph_2SnCl_2 (3.55 $mm.sec^{-1}$ and 2.82 $mm.sec^{-1}$ respectively, Table 32, ref. 4) strongly suggesting that the Me compound is somewhat associated, while the Ph compound is unassociated. The unassociated structure has been confirmed by an X-ray study[37], but there appears to be disagreement amongst crystallographers as to whether Me_2SnCl_2 is associated[37,38]. The associated nature of Me_2SnCl_2 should be confirmed by frozen solution Mössbauer studies.

TABLE 10
Quadrupole splittings for the five $Fe(CO)_2[P(Me)_3]_2I_2$ isomers[22]

	Quadrupole splitting ($mm.sec^{-1}$)		η
	Predicted	Observed	Predicted
1 *trans* P *cis* I and CO	−0.96	0.90	0
2 all *trans*	+1.31	+1.31	0.52
3 all *cis*	−0.65		0.52
4 *trans* I *cis* P and CO	+1.26		0
5 *trans* CO *cis* I and P	−0.30		0

TABLE 11
Some Sn^{IV} quadrupole splitting data[4] ($mm.sec^{-1}$ at 80° K)

X	F	Cl	Br	I
Me_3SnX	3.82	3.44	3.39	3.10
Ph_3SnX	3.53	2.56	2.25	2.25

The quadrupole splittings have been used to detect association in a host of other Sn^{IV} compounds [4,33,39].

(iii) Prediction of other quadrupole parameters and NMR linewidths

The next major use of PQS values – and one which takes the method into a large number of non-Mössbauer elements – is for predicting the signs and magnitudes of e^2qQ for other t_{2g}^6 ions such as Mn^I, Co^{III}, Ru^{II}, W^0; and $4d^{10}$ ions such as Sb^V (refs. 40–42). Mn, Co (and such elements as V and Re) have NQR isotopes[11], but the signs of the quadrupole splitting cannot be obtained for these elements or for the Mössbauer isotope ^{99}Ru. Molecular orbital calculations have been carried out for some Mn^I (refs. 42, 43) and Co^{III} compounds (refs. 43, 44), and the orbital populations derived from these calculations have been used to predict $(e^2qQ)_{^{55}Mn}$ and $(e^2qQ)_{^{59}Co}$. These signs appear to be incorrect.

We assume that in isoelectronic and isostructural compounds such as $[Me_3SnCl_2]^-$ and Me_3SbCl_2 or *trans*-$[Co^{III}(NH_3)_4Cl_2]^+$ and "*trans*-$Fe(NH_3)_4Cl_2$" that the bonding is identical, and we can then write

$$(e^2qQ)_{Co\ cpd} = \left[\frac{q_{3d(Co)}Q_{^{59}Co}}{q_{3d(Fe)}Q_{^{57}Fe}}\right](e^2qQ)_{Fe\ cpd} \qquad (9)$$

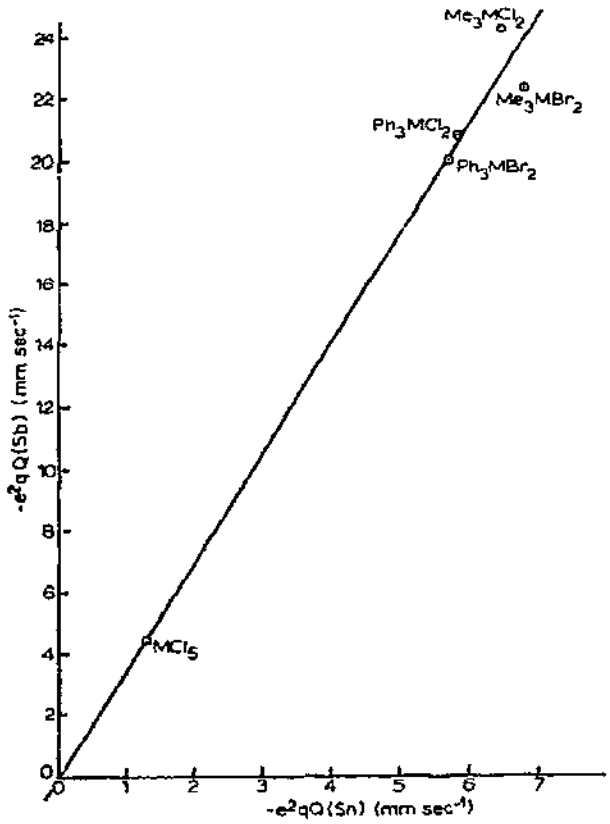

Fig.4. e^2qQ for Sb^V compounds plotted against e^2qQ for isoelectronic, isostructural Sn^{IV} compounds. (The tin species carry net negative charges.)

and analogous expressions could be written for Sn^{IV}–Sb^V and Fe^{II}–Ru^{II} compounds. There are a few ways of using this formula. For a number of compounds we can plot one quadrupole splitting versus the other and we should obtain a straight line with zero intercept, with the slope given by the square bracketed term in eqn. (9). If the q's are known and one of the Q's, we can obtain the sign and magnitude of the other Q. For example (Fig.4), for Sn and Sb species we obtain an excellent straight line whose slope gives $Q_{^{119}Sn} = -0.062$ barn[41]. This is in excellent agreement with another recently determined value[46] of −0.065 barn. From the correlation, it is interesting to note that the sign of e^2qQ for $SnCl_5^-$ must be negative. This quadrupole splitting was too small for the sign to be measured experimentally. A similar plot for Ru compounds, using the PQS values to predict the quadrupole splittings for the hypothetical Fe analogues, gave $|Q_{^{99}Ru}| = 0.34$ barn (ref. 41).

If very few quadrupole splittings are known, as is the case for Co^{III} compounds, one of the Q's can be solved for from just one or two compounds. For example, from the measured e^2qQ for *trans*-$Co(NH_3)_4Cl_2^+$ species[44] and the calculated quadrupole splitting from PQS values (Table 6) for "*trans*-$Fe(NH_3)_4Cl_2$", we calculated [40] $|Q_{^{57}Fe}| = 0.16$ barn and showed that the sign of q in both compounds should be positive, in opposition to the neg-

ative sign predicted from MO calculations[44]. The value of $|Q_{^{57}Fe}|$ is in reasonable agreement with the value of 0.20 generally accepted (references cited in ref. 40).

Alternatively, we can use eqn. (9) to calculate e^2qQ for an isoelectronic, isostructural compound if the q's and Q's are known and $(e^2qQ)_{\text{Fe cpd}}$ can be obtained either by direct measurement or from the PQS values. For example, consider the $^{55}Mn^{I}$ e^2qQ values in Table 12 obtained from NMR measurements. The signs for these splittings could not be obtained experimentally. The signs in brackets are predicted from MO calculations. From the PQS values in Table 6, the e^2qQ values for the $[Fe(CO)_5L]^+$ ($L = Cl^-, Br^-, I^-, SnCl_3^-, H^-$) analogues were predicted, and using known values[42] for the q's and Q's*, eqn. (9) was used to obtain the e^2qQ values for the Mn compounds in Table 12. The signs are opposite to those predicted previously, and the magnitudes of e^2qQ are in remarkably good agreement with the observed considering the assumptions involved in the PQS treatment, and possible errors in the q's and Q's.

TABLE 12
e^2qQ for Mn^{I} compounds

Compound	e^2qQ (MHz)	
	Observed[20,48]	Predicted[42]
$Mn(CO)_5Cl$	(−)13.86	+16.2
$Mn(CO)_5Br$	(−)17.46	+17.5
$Mn(CO)_5I$	(−)19.85	+16.8
$Mn(CO)_5SnCl_3$	(−) 7.3	+ 7.8
$Mn(CO)_5H$		−31.7

The above results are perhaps of greater interest, because we can now use the predicted e^2qQ values to rationalize trends in ^{55}Mn NMR linewidths. The linewidth for a quadrupolar nucleus ΔH can be expressed[49]

$$\Delta H = C\left(\frac{e^2qQ}{h}\right)^2 \tau_c \qquad (10)$$

where C = constant, and τ_c = rotational correlation time, which depends mostly on the size of the molecule, the type of solvent and solvent–solute interactions.

Since NMR linewidths for such $I > \frac{1}{2}$ nuclei are determined mainly by quadrupole relaxation[49], $\sqrt{\Delta H}$ should be proportional to e^2qQ. There is good qualitative agreement between the observed relative ΔH values[50,51] and those expected from the calculated (e^2qQ) values in Table 12. Thus the observed linewidths for the $Mn(CO)_5X$ compounds are (in gauss): $Mn(CO)_5SnCl_3$ = 0.18, $Mn(CO)_5Cl$ = 0.18, $Mn(CO)_5Br$ = 0.38, $Mn(CO)_5I$ = 0.557 and $Mn(CO)_5H$ = 2.39 (ref. 50). Also the observed $\sqrt{\Delta H}$ versus chemical shift correlations[51] strongly suggest that there should be a change in sign of e^2qQ from the

* $Q_{^{55}Mn}$ is taken to be positive.

$Mn(CO)_5L$ (L = Cl, Br, $SnCl_3$) compounds to $Mn(CO)_5H$ as predicted above. This correlation also strongly suggests that all $Mn(CO)_5L$ compounds with chemical shifts below ~ 2150 p.p.m. have positive e^2qQ values, while those having chemical shifts above this value have negative e^2qQ values.

Values for PQS and eqn. (9) should now be useful for predicting quadrupole parameters for other species such as $^{182}W^0$ and $^{193}Ir^{III}$, as well as for correlating and predicting future $^{99}Ru^{II}$, $^{59}Co^{III}$ and $^{55}Mn^{I}$ quadrupole splittings.

(iv) Bonding properties of ligands and preparation of new compounds

Finally, we come to what is probably the most important information obtainable from PQS values – bonding information. Just as the quadrupole splittings for the *trans*-$[FeHL(depe)_2]^+$ series (Fig.3) become more negative with increasing $(\sigma - \pi)$ properties of ligand L, so the PQS values become more negative with increasing $(\sigma - \pi)$ (ref. 5)*. Similarly, partial center shift (PCS) values can be calculated[5] and like the center shift, PCS $\alpha -(\sigma + \pi)$. A plot of PCS versus PQS[22] for a large number of neutral ligands (Fig.5) is similar in form to the CS–QS plot in Fig.3. Most of the ligands lie close to the line drawn, again indicating that σ effects dominate both the CS and QS. The stronger the π acceptor, the farther the ligand lies to the left of the line.

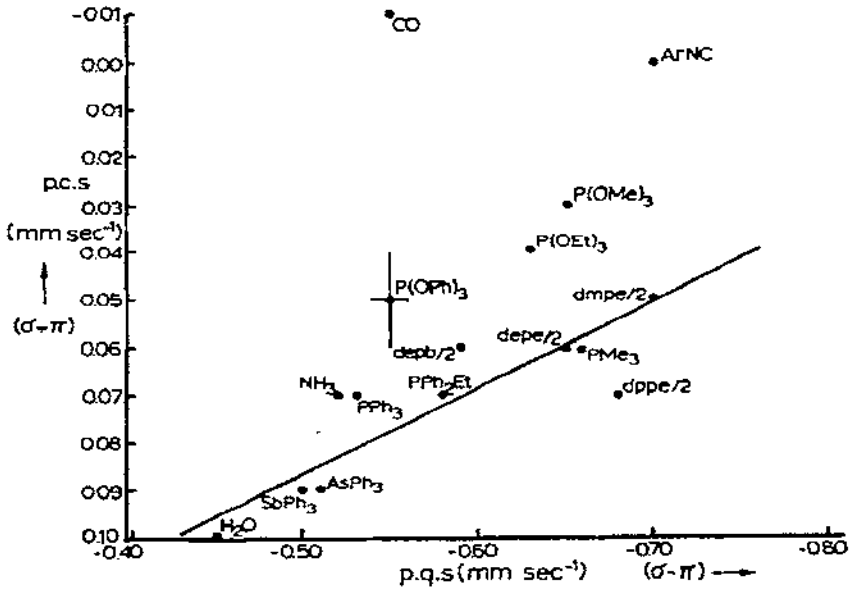

Fig.5. Plot of partial center shift (PCS) versus partial quadrupole splitting (PQS) for neutral ligands bonded to Fe^{II}. The errors on both are > 0.01 mm.sec^{-1} represented by the bars on the $P(OPh)_3$ position.

* Clark et al.[34] have developed a formal molecular orbital model to account for the additivity considering σ bonding. Their results indicate that π bonding contributions may not be additive.

Thus CO is a very strong σ donor and π acceptor, and phosphites are stronger π acceptors than their corresponding phosphines.

We would now like to use the above bonding information to prepare new compounds. A host of Fe^{II} isocyanide compounds have been prepared[52], but very few six-coordinate Fe^{II} compounds containing phosphites or phosphines are known, and all of these known phosphine and phosphite compounds[32] contain the powerful ligands H or CO. Yet our bonding information from Fig.5 suggests that $P(OMe)_3$ is nearly as good a σ and π ligand as are isocyanides, suggesting that $P(OMe)_3$ compounds analogous to the isocyanide derivatives should be capable of being prepared if steric factors are not important.

A number of the $P(OMe)_3$ analogues have now been made[53], and a selection of these are listed in Table 13 along with their Mössbauer parameters – neutral compounds, monocations and dications. It is apparent then that the bonding information derivable from Mössbauer parameters should be very useful in preparing compounds of Fe^{II}, and other ions such as Mn^{I} and Co^{III} having $(t_{2g})^6$ electronic configurations.

TABLE 13
Comparison of $P(OMe)_3$ and ArNC complexes[53]

Compound	CS ($mm.sec^{-1}$)	QS ($mm.sec^{-1}$)
cis-$FeClSnCl_3[P(OMe)_3]_4$	0.34	(−)0.45
$\{FeSnCl_3[P(OMe)_3]_5\}BPh_4$	0.34	(+)0.36
$\{Fe[P(OMe)_3]_6\}(BPh_4)_2$	0.30	<0.10
$Fe(CO)_3I_2[P(OMe)_3]$	0.29	0.36
$Fe(CO)_2Br_2[P(OMe)_3]_2$	0.29	(−)0.93
cis-$FeClSnCl_3[ArNC]_4$	0.34	(−)0.67
$[FeSnCl_3(ArNC)_5]ClO_4$	0.22	(+)0.33
$[Fe(CNMe)_6](HSO_4)_2$	0.23	0
$Fe(CO)_3I_2(ArNC)$	0.29	0.58
$Fe(CO)_2I_2(ArNC)_2$	0.29	(−)0.79

ACKNOWLEDGEMENTS

I am very grateful to all my co-workers mentioned in the references, both at the University of Cambridge and the University of Western Ontario. I am also grateful to the National Research Council of Canada for financial support and the award of the E.W. Steacie Fellowship.

REFERENCES

1 R.L. Mössbauer, *Naturwissenschaften*, 45 (1958) 538.
2 A.H. Muir, K.J. Ando and H.M. Coogan (Eds.), *Mössbauer Effect Data Index*, Wiley, New York, 1966.
3 T.C. Gibb and N.N. Greenwood, *Mössbauer Spectroscopy*, Chapman and Hall, London, 1971.
4 G.M. Bancroft and R.H. Platt, *Advan. Inorg. Chem. Radiochem.*, 15 (1972) 59.

5 G.M. Bancroft, M.J. Mays and B.E. Prater, *Discuss. Faraday Soc.*, 47 (1969) 136; *J. Chem. Soc. A*, (1970) 956.
6 R.V. Parish and R.H. Platt, *J. Chem. Soc. A*, (1969) 2145; *Inorg. Chim. Acta*, 4 (1970) 65.
7 M.G. Clark, *Mol. Phys.*, 20 (1971) 257.
8 A.J.F. Boyle and H.E. Hall, *Rep. Progr. Phys.*, 25 (1962) 441.
9 H. Frauenfelder, *The Mössbauer Effect*, Benjamin, New York, 1962.
10 R. Ingalls, *Phys. Rev. A*, 133 (1964) 787.
11 E.A.C. Lucken, *Nuclear Quadrupole Coupling Constants*, Academic Press, New York, 1969.
12 M.G. Clark, G.M. Bancroft and A.J. Stone, *J. Chem. Phys.*, 47 (1967) 4250.
13 R.L. Collins, *J. Chem. Phys.*, 42 (1965) 1072.
14 T.C. Gibb, *J. Chem. Soc. A*, (1970) 2503.
15 G.M. Bancroft, M.J. Mays, B.E. Prater and F.P. Stefanini, *J. Chem. Soc. A*, (1970) 2146.
16 G.M. Bancroft, R.E.B. Garrod, A.G. Maddock, M.J. Mays and B.E. Prater, *J. Amer. Chem. Soc.*, 94 (1972) 647.
17 J. Chatt, D.P. Melville and R.L. Richards, *J. Chem. Soc. A*, (1969) 2841.
18 R.F. Bryan, *J. Chem. Soc. A*, (1968) 696; H.P. Weber and R.F. Bryan, *Chem. Commun.*, (1966) 443.
19 E.S. Mooberry, H.W. Spiess and R.K. Sheline, *J. Chem. Phys.*, 57 (1972) 813.
20 J.L. Slater, M. Pupp and R.K. Sheline, *J. Chem. Phys.*, 57 (1972) 2105.
21 G.M. Bancroft, R.E.B. Garrod and A.G. Maddock, *J. Chem. Soc. A*, (1971) 3165.
22 G.M. Bancroft and E.T. Libbey, *J. Chem. Soc. Dalton*, to be published.
23 D.H. Busch, private communication; M.J. Mays, private communication.
24 M.G. Clark, A.G. Maddock and R.H. Platt, *J. Chem. Soc. Dalton*, (1972) 281.
25 G.M. Bancroft, K.D. Butler, A.T. Rake and B. Dale, *J. Chem. Soc. Dalton*, (1972) 2025.
26 G.M. Bancroft, K.D. Butler and A.T. Rake, *J. Organometal. Chem.*, 34 (1972) 137.
27 M.G. Clark, *Chem. Phys. Lett.*, 13 (1972) 316.
28 R.V. Parish and C.E. Johnson, *J. Chem. Soc. A*, (1971) 1906.
29 B.A. Goodman, N.N. Greenwood, K.L. Jaura and K.K. Sharma, *J. Chem. Soc. A*, (1971) 1865.
30 R.R. Berrett and B.W. Fitzsimmons, *J. Chem. Soc. A*, (1967) 525.
31 B.W. Fitzsimmons, N.J. Seeley and A.W. Smith, *J. Chem. Soc. A*, (1969) 143; (1970) 935.
32 G.M. Bancroft and E.T. Libbey, *Can. J. Chem.*, 51 (1973) 1482.
33 A.G. Maddock and R.H. Platt, *J. Chem. Soc. A*, (1971) 1191.
34 H.C. Clark, R.J. O'Brien and J. Trotter, *J. Chem. Soc., London*, (1964) 2332.
35 A.G. Davies, personal communication to R.H. Platt.
36 N.G. Bokii, G.N. Zakharova and Yu.T. Struchkov, *J. Struct. Chem. (USSR)*, 11 (1970) 828; *Zh. Strukt. Chim.*, 11 (1970) 895.
37 P.T. Greene and R.F. Bryan, *J. Chem. Soc. A*, (1971) 2549.
38 A.G. Davies, H.J. Milledge, D.C. Puxley and P.J. Smith, *J. Chem. Soc. A*, (1970) 2862.
39 R.V. Parish, *Progr. Inorg. Chem.*, 15 (1972) 101.
40 G.M. Bancroft, *Chem. Phys. Lett.*, 10 (1971) 449.
41 G.M. Bancroft, K.D. Butler and E.T. Libbey, *J. Chem. Soc. Dalton*, (1972) 2643.
42 G.M. Bancroft, H.C. Clark, R.G. Kidd, A.T. Rake and H.G. Spinney, *Inorg. Chem.*, 12 (1973) 728.
43 R.F. Fenske and R.L. De Kock, *Inorg. Chem.*, 9 (1970) 1053.
44 H.W. Spiess, H. Haas and H. Hartman, *J. Chem. Phys.*, 50 (1969) 3057.
45 C.B. Harris, *J. Chem. Phys.*, 49 (1968) 1648.
46 H. Micklitz and P.H. Barrett, *Phys. Rev. B*, 5 (1972) 1704.
47 I. Watanabe and Y. Yamagoto, *J. Chem. Phys.*, 46 (1967) 407.
48 H.W. Spiess and R.K. Sheline, *J. Chem. Phys.*, 54 (1971) 1099.
49 A.A. Abragam, *The Principles of Nuclear Magnetism*, Oxford University Press, Oxford, 1962, Chap. 8.
50 F. Calderazzo, E.A.C. Lucken and D.F. Williams, *J. Chem. Soc. A*, (1967) 154.
51 S. Onaka, T. Mujamoto and Y. Sasaki, *Bull. Chem. Soc. Jap.*, 44 (1971) 1851.
52 M.J. Mays and B.E. Prater, *J. Chem. Soc. A*, (1969) 2525 and references therein.
53 G.M. Bancroft and E.T. Libbey, *J. Chem. Soc. Dalton*, in press.